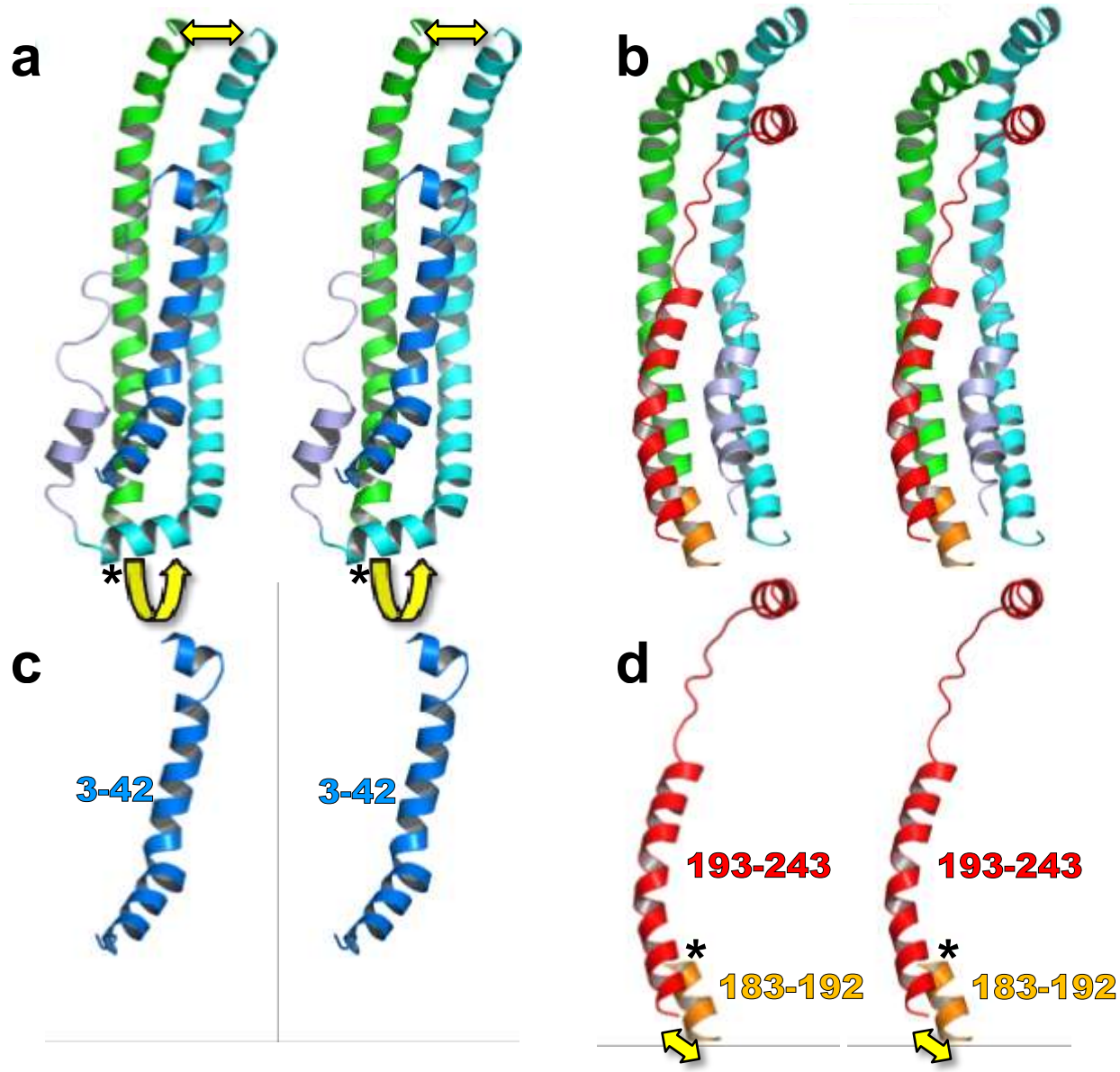

Fig. S1. Initial monomers created from different chains of two crystal structures, C-terminally truncated (Δ185-243)apoA-I and N-terminally truncated (Δ1-43)apoA-I. a. Relaxed-eye stereo view of initial monomer created from C-terminally truncated (Δ185-243)apoA-I. Residues 3-42, blue; residues 43-67, purple; residues 68-130, cyan; residues 131-182, green. Residues 3-130 are from Chain A and residues 131-182 are from Chain B. Yellow double headed arrow denotes joining of residue 130 to 131 to complete helical repeat 5 hairpin. Yellow arrow hairpin denotes where missing residues after 182 wrap around helical segment 71-80 at the bottom. * denotes where residue182 joins with 183 in (d). **b.** Relaxed-eye stereo view of initial monomer created from N-terminally truncated (Δ1-43)apoA-I. Residues 43-67 (Chain A), purple; residues 68-130 (Chain D), cyan; residues 131-182 (Chain C), green; residues 183-192 (Chain C), orange; residues 193-243 (Chain B), red. **c.** Relaxed-eye stereo view of residues 3-42 from (Δ185-243)apoA-I (Chain A) isolated from (a) and missing in (b). **d.** Relaxed-eye stereo view of residues 183-243 from (Δ1-43)apoA-I (Chains C and B) isolated from (b) and missing in (a). The yellow arrow shows where a hairpin turn is required to join residue 192 to 193. * denotes where residue183 joins with 182 in (a).

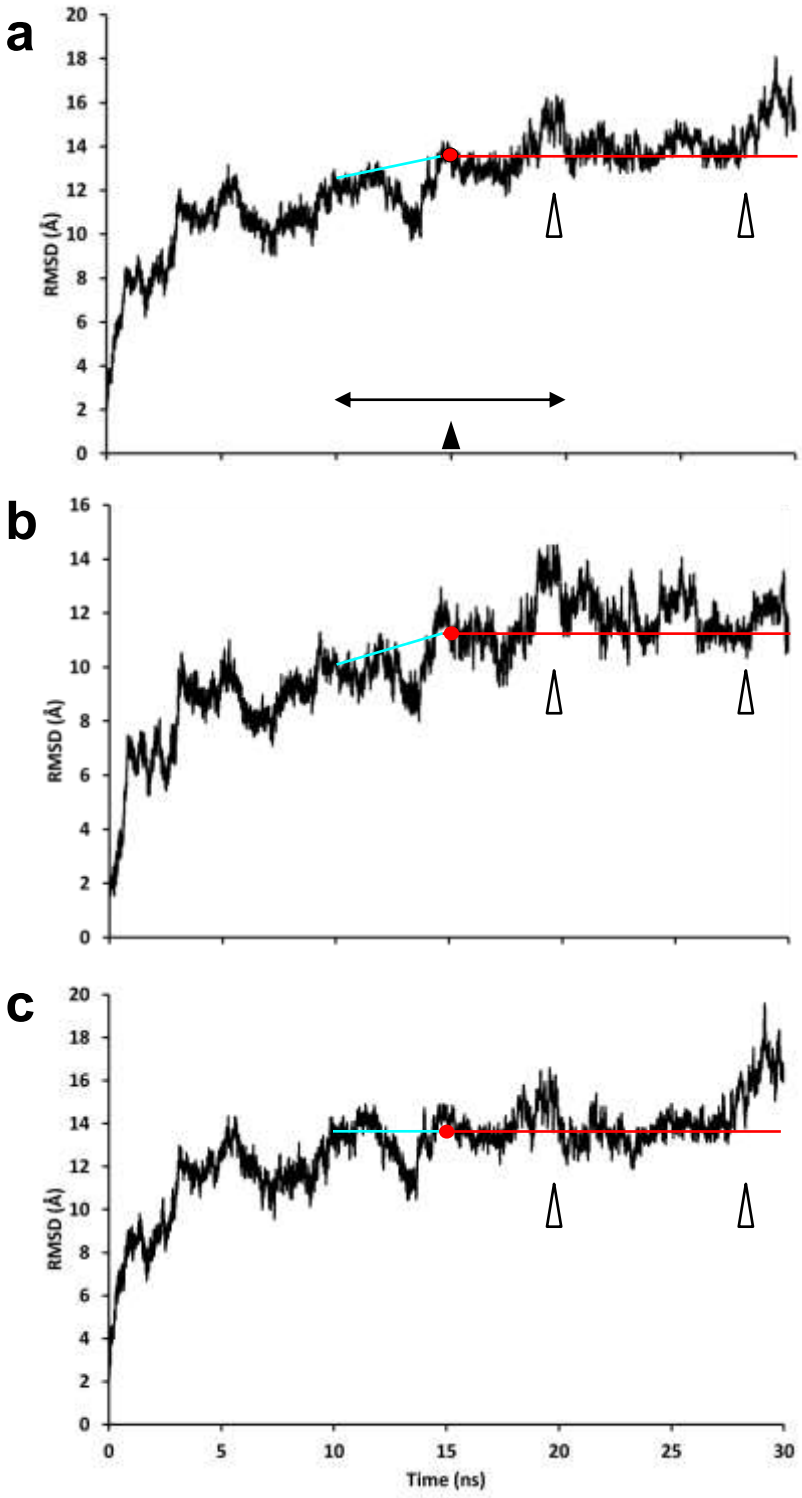

Fig. S2. Plots of changes in RMSD of the initial crystal model during 30 ns of MD simulation at 500 K. 10-15 ns trend line, cyan; 15-30 ns trend line, red. **a.** RMSD of the Cα of all residues plotted over time of simulation. Open arrowheads, RMSD changes induced by open structures. Double arrow, 10–20 ns interval. Closed arrowhead, 15 ns simulation. **b.** RMSD of the Cα of the CH domains 1, 4 and 5 (residues 7-44, 81-115 and 147-178) **c.** RMSD of the Cα of all non-CH domains, which includes several helical regions.

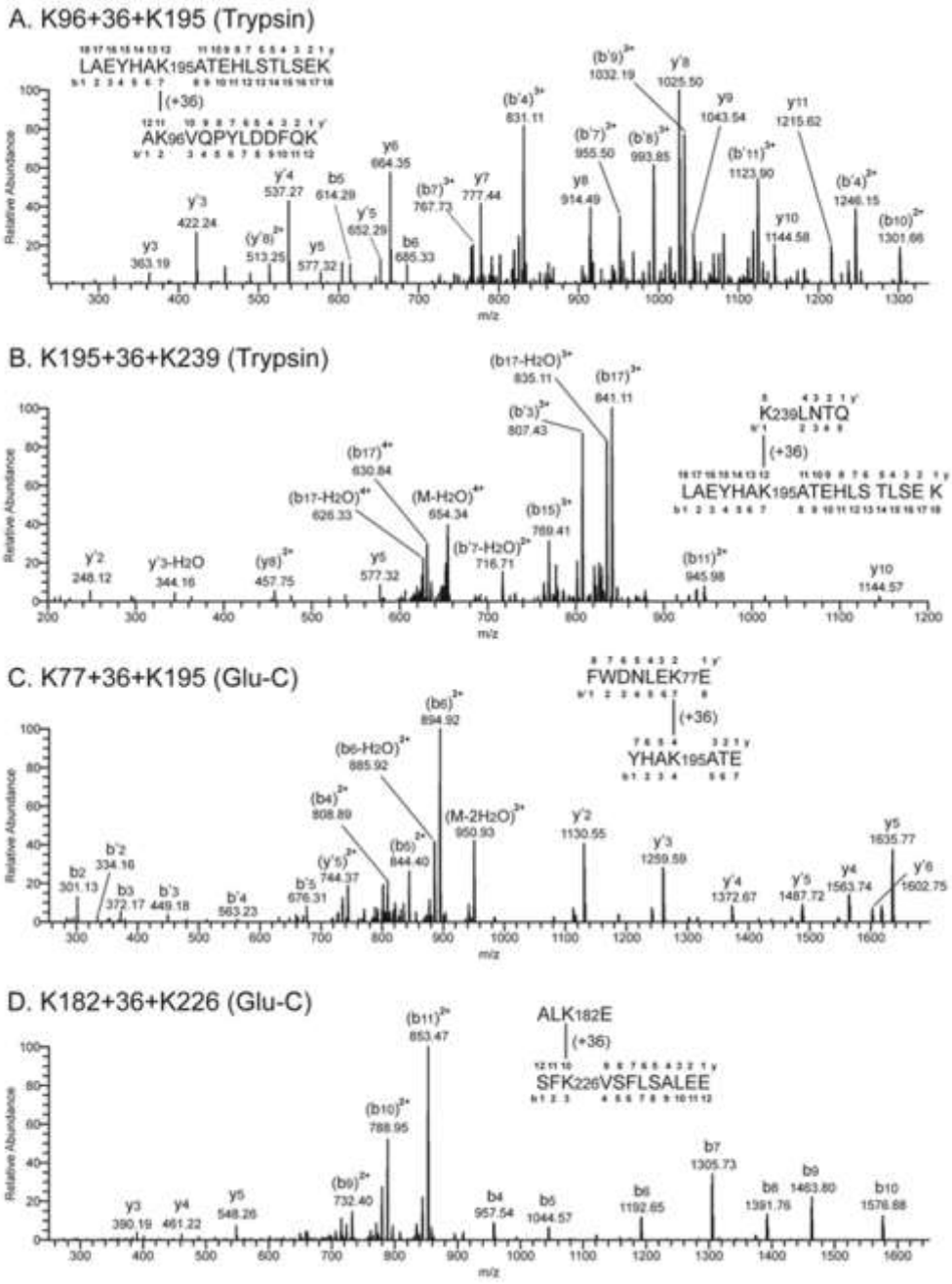

Fig. S3. MS/MS analysis of Lys-MDA-Lys (K+36+K) in MDA-modified apoA-I. Lipid-free apoA-I was exposed to a 20-fold molar excess of MDA. Glu-C peptide digest and trypsin peptide digests were analyzed by LC-ESI-MS/MS, as described in Methods. (A) MS/MS spectrum of peptides consisting of L189-K206 and A95-K106 containing an inter-peptide MDA link (36 amu) between K195 and K96. (B) MS/MS spectrum of peptides consisting of L189-K206 and K239-Q243 containing an inter-peptide MDA link between K195 and K239. (C) MS/MS spectrum of peptides consisting of F71-E78 and Y192-E198 containing an inter-peptide MDA link between K77 and K195. (D) MS/MS spectrum of A180-E183 and S224-E235 containing an inter-chain MDA link between K182 and K226.

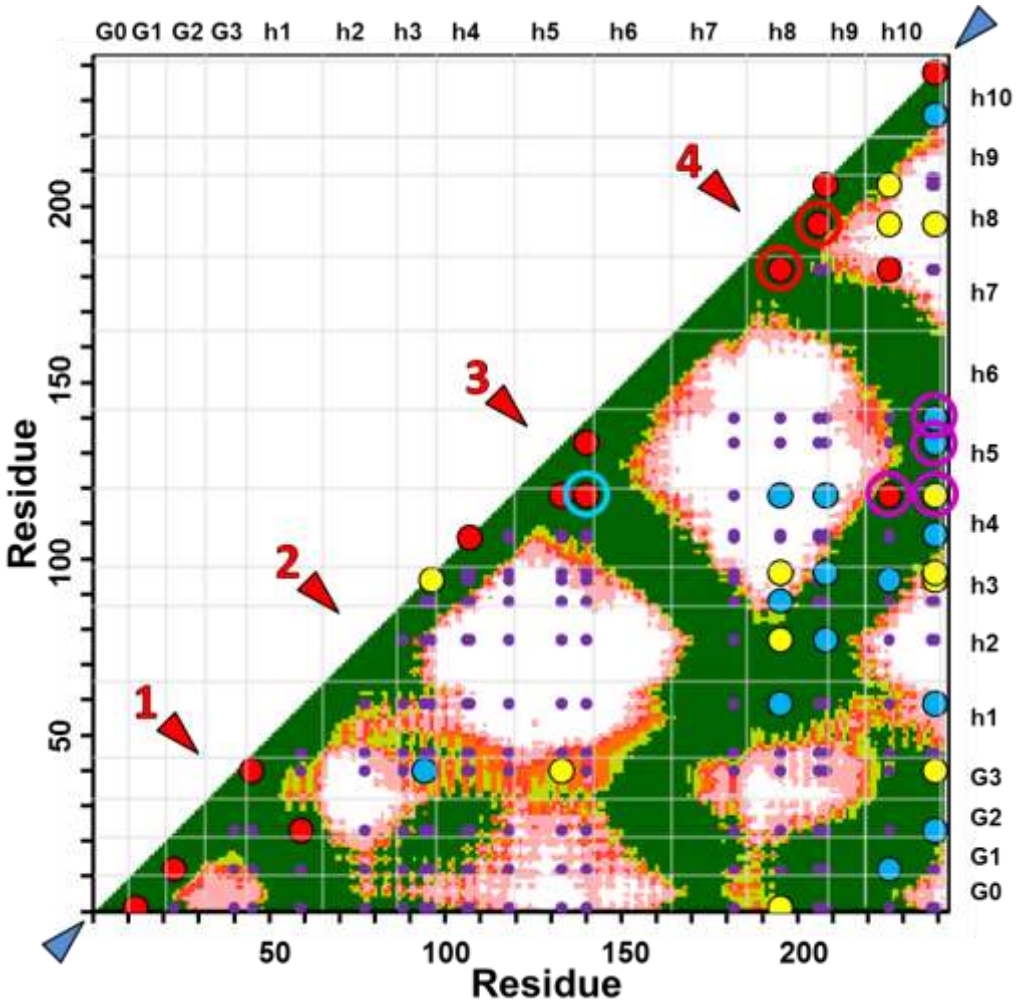

Fig. S4. Overlay of 41 chemical cross-linking data points onto the contact map plot of Cα distances ≤ 23 Å for the full trajectory of the 30 ns MD simulation. Small purple circles represent the position of all potential cross-links. Red circles, most probable one-third of cross-links; yellow circles, median probable one-third of cross-links; blue, least probable one-third of cross-links. Red arrowheads, loops and turns; blue arrowheads, N- and C-termini. Bulls' eyes, same as in **Fig. 4b**.

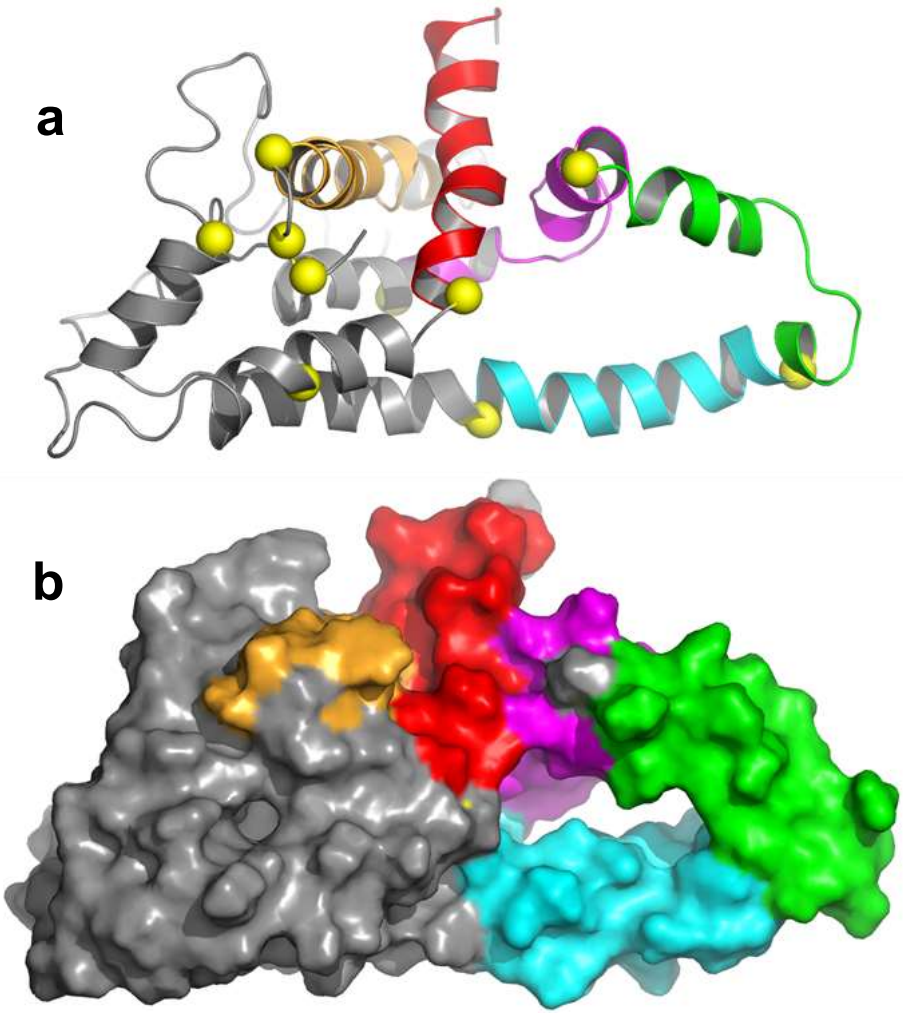

Fig. S5. Depth cued molecular graphics representation of the 30 ns structure. CH1, gold; H4, cyan; H5, green; H6, magenta; H10, red. **a.** Ribbons model. **b.** Surface representation.

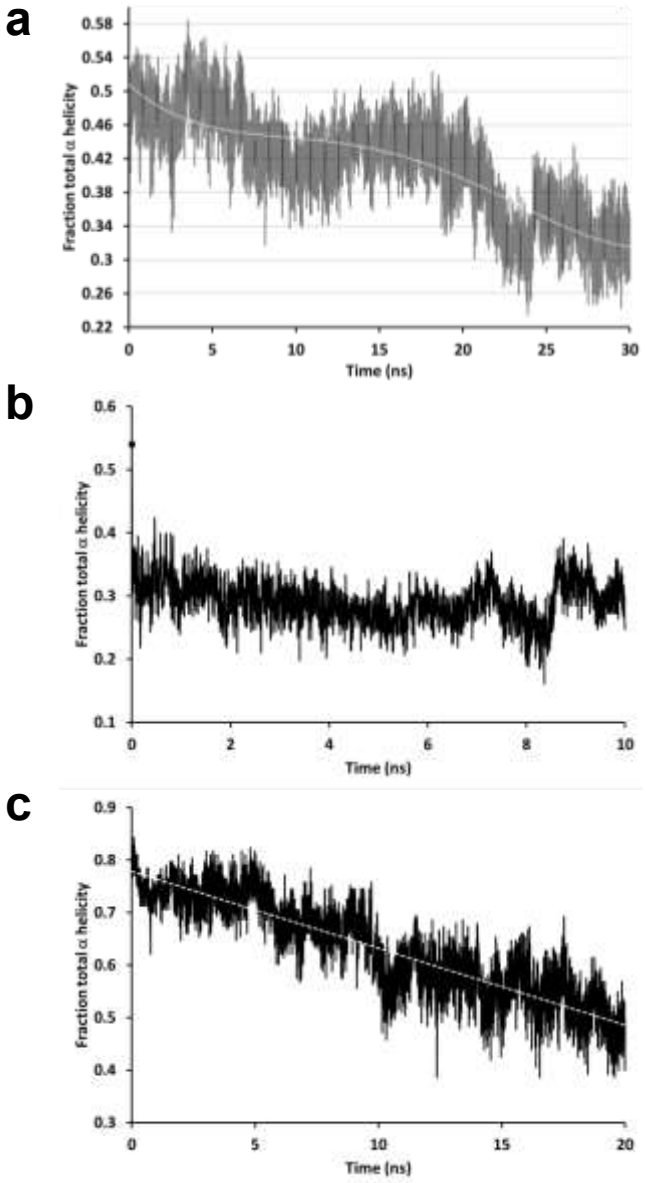

Fig. S6. Plots of changes in helicity of two published monomeric apoA-I models and one control four helix bundle apolipoprotein during MD simulation at 500 K. a. Change in fraction total α helicity during 30 ns MD simulation of model Silva [1]. **b.** Change in fraction total α helicity during 10 ns MD simulation of model Pollard [2]. **c.** Change in fraction total α helicity during 20 ns MD simulation of the four helix bundle apolipophorin III crystal structure [3].

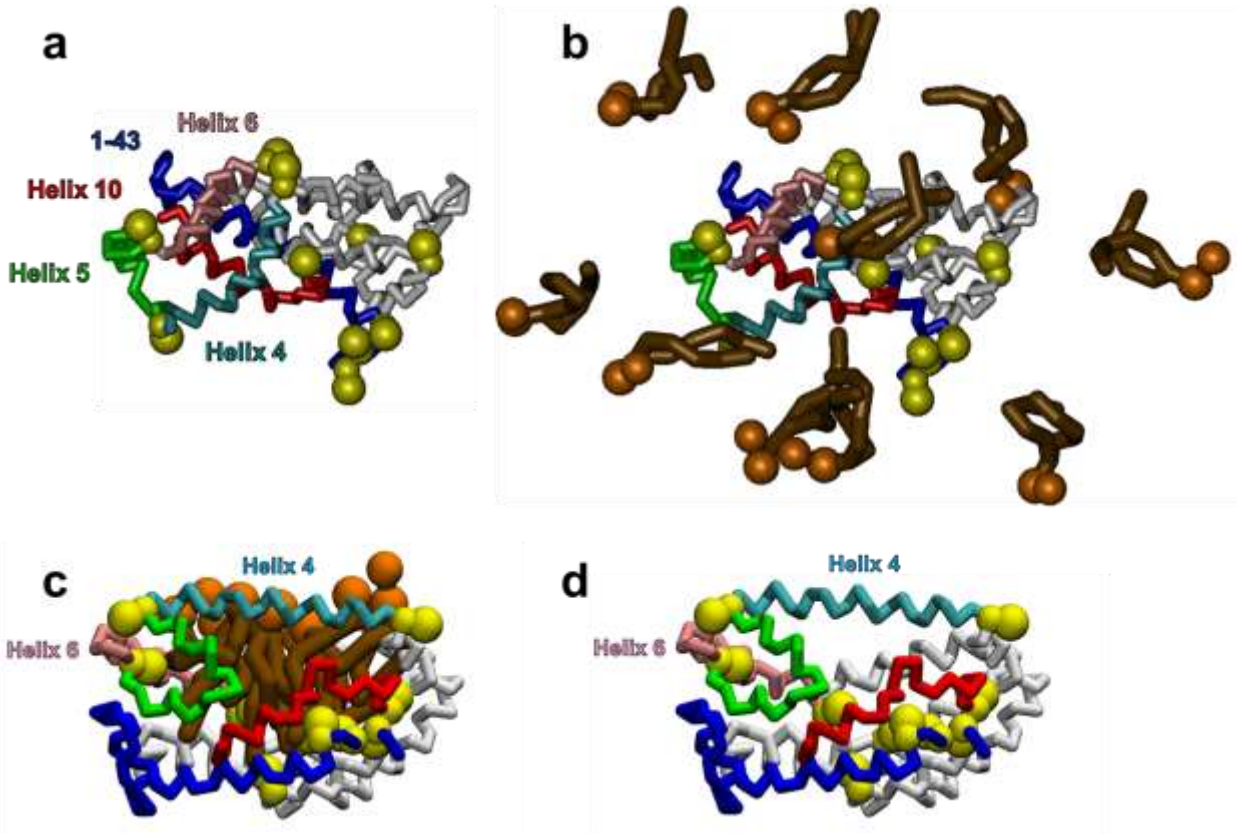

Fig. S7. "Cup" model derived by coarse grained MD simulation of interaction of PL with lipid-free apoA-I monomer. Course grained (CG) apoA-I monomer with flexible secondary structure and CG POPC simulated as described [4]. **a.** CG model of "best" lipid-free apoA-I monomer model (15ns structure in **Fig. 6**). **b.** CG 15ns model in periodic box containing 10 randomly distributed monomeric POPC. **c.** Result after 20 μs CG MD simulation showing uptake of 7 CG POPC to form a "cup"-shaped lipid-poor particle. **d.** Same as (c) minus POPC.

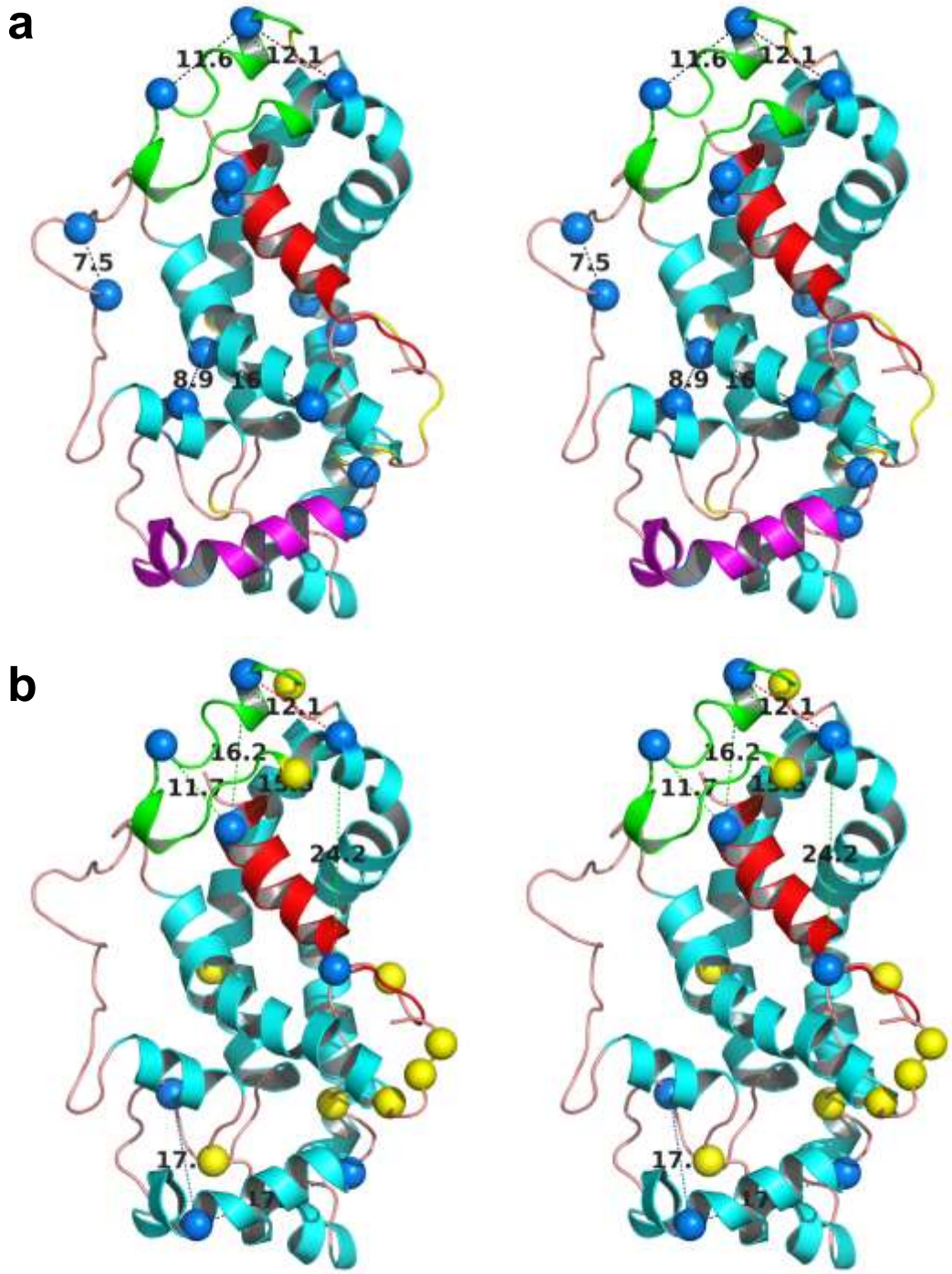

Fig. S8. Location of key cross-links on relaxed-eyed stereo ribbons representations of the 15 ns model. H5, green; H10, red. **a.** Five non-trivial cross-links common to Silva, et al [1], Pollard, et al [2] and this study (black dotted lines). All lysine residues involved in common cross-links, blue spheres. **b.** Cross-links that define the H5-H10 contact model. All fourteen lysine residues involved in common cross-links, blue spheres. Cross-links denoting: H5 hairpin, red dotted line; H5-H10 contact, green dotted lines; Y192 loop/hairpin, blue dotted lines.

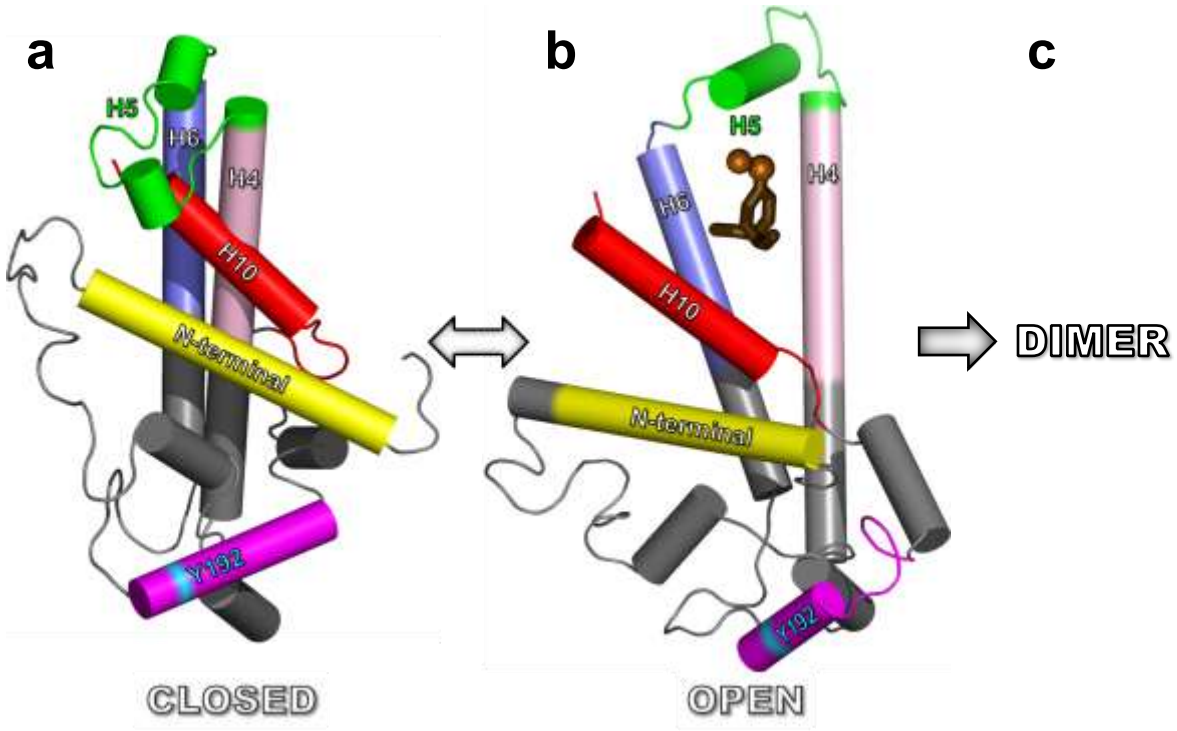

Figure S9. Cartoon representation of a dynamic model for formation of discoidal HDL driven by the cycling of lipid-free monomeric human apoA-I between closed and open states. H4, peach; H5, green; H6, steel blue; H10, red; N-terminal helix, yellow; Y192, cyan; Y192 loop/helix, magenta. **a.** Closed (15 ns) model. **b.** Open (20 ns) model in which the tandem helical repeats, H4, H5, H6 and H10 open to form a hydrophobic pocket called a "lipid cup". A CG PC molecule (brown and gold) symbolizes lipid being taken up by the "lipid cup" to form lipid-poor apoA-I. **c.** Dimerization of lipid-poor apoA-I initiated through antiparallel pairwise H4-H6 hairpin interactions to form discoidal HDL.

Table S1

Comparison of Cross-links of Silva, et al [1] and Pollard, et al [2] with those of this study

Lys1	Lys2	Silva	Pollard	This study
1α	12		y	y
1α	59		y	
1α	96	y		
1α	118		y	
1α	195			y
12	**23**	**y**	**y**	**y**
12	195		y	
12	226			y
23	**59**	**y**	**y**	**y**
23	239			y
40	**45**	**y**	**y**	**y**
40	59		y	
40	94			y
40	118		y	
40	133		y	y
40	140		y	
40	182		y	
40	239		y	y
45	59		y	
59	195			y
59	239			y
77	195			y
77	208			y
88	94	y	y	
88	118		y	
88	195			y
94	**96**	**y**	**y**	**y**
94	208	y		
94	226			y
94	226			y
94	239		y	y
96	106	y	y	
96	195	y		y
96	208	y		y
96	226	y		
96	239			y
106	107	y		y
107	239			y
118	133		y	y
118	**140**	**y**	**y**	**y**
118	195			y
118	208			y
118	**226**			**y**
118	**239**			**y**
133	**140**	**y**	**y**	**y**
133	**239**			**y**
140	**239**			**y**
182	**195**			**y**
182	226			y
195	**206**			**y**
195	226			y
195	239			y
206	**208**	**y**	**y**	**y**
206	226			y
226	238	y		
226	239			y
238	**239**	**y**	**y**	**y**
Total		**17**	**24**	**41**

1α, N-terminal amino group; gray shading, cross-links common to all three studies; red, evidence for H5 hairpin; green, evidence for contact of H5 with H10; blue, evidence for Y192 loop/hairpin.

References

[1] Silva, R. A., Hilliard, G. M., Fang, J., Macha, S., and Davidson, W. S. (2005) A three-dimensional molecular model of lipid-free apolipoprotein A-I determined by cross-linking/mass spectrometry and sequence threading, *Biochemistry 44*, 2759-2769.

[2] Pollard, R. D., Fulp, B., Samuel, M. P., Sorci-Thomas, M. G., and Thomas, M. J. (2013) The conformation of lipid-free human apolipoprotein A-I in solution, *Biochemistry 52*, 9470-9481.

[3] Breiter, D. R., Kanost, M. R., Benning, M. M., Wesenberg, G., Law, J. H., Wells, M. A., Rayment, I., and Holden, H. M. (1991) Molecular structure of an apolipoprotein determined at 2.5-A resolution, *Biochemistry 30*, 603-608.

[4] Segrest, J. P., Jones, M. K., and Catte, A. (2013) MD simulations suggest important surface differences between reconstituted and circulating spherical HDL, *J Lipid Res 54*, 2718-2732.